GAMMA REMOTE SENSING

SENTINEL-1 SUPPORT IN THE GAMMA SOFTWARE

Urs Wegmüller, Charles Werner, Tazio Strozzi, Andreas Wiesmann, Othmar Frey, and Maurizio Santoro
Gamma Remote Sensing, CH- 3073 Gümligen, Switzerland
http://www.gamma-rs.ch

Abstract

First Sentinel-1 (S1) SAR results look promising but InSAR processing is challenging because of the special TOPS mode [1] used to acquire the Interferometric Wide-Swath (IWS) data. The steep azimuth spectra ramps in each burst result in very stringent co-registration requirements. Combining the data of the individual bursts and sub-swaths into consistent mosaics requires careful "book-keeping" in the handling of the data and meta data and the large file sizes and high data throughputs require a good performance. Considering these challenges getting adequate support from software gets increasingly important. In this contribution we describe the Sentinel-1 support in the GAMMA Software, a high-level software package used by researchers, service providers and operational users in their SAR, InSAR and PSI work.

S1 IWS data handling and basic functionality

Currently the GAMMA Software supports the use of S1 IWS SLC (Single Look Complex) and GRD (Ground Range Dataset) products. The GRD products can be imported, calibrated and geocoded in the GAMMA Software. The GRD products may be used to analyze the backscattering coefficient and for offset tracking, e.g. to map glacier motion.

The **S1 IWS SLC** product is a set of three "burst SLC", each one including a number of SLCs obtained by processing the bursts over one of the IWS sub-swaths. An example of a burst SLC of sub-swath IW1 is shown in Figure 1. The area covered by the individual bursts overlaps in both azimuth (between sub-sequent bursts) and range (between neighboring sub-swaths), as sketched in Figure 2. In the GAMMA Software the S1 IWS SLC product is imported and stored as "burst SLC" consisting of the image data of the 3 sub-swaths and related parameter files containing the relevant metadata. In the importing, the radiometric calibration is applied. Functionality to process the "burst SLC" includes the possibility to generate mosaic SLC and a mosaic MLI (multi-look detected image, Figure 3). In both cases, this is a single data file with a single parameter file. The data is cut in the overlap region such that only pixels (looks) from the same burst and sub-swath are combined into a MLI pixel. Geometrically and radiometrically the S1 IWS SLC are on a very high standard, so that the generated mosaics are typically seamless in both range and azimuth. The Doppler Centroid of the data varies strongly along-track, which is very relevant for the SLC co-registration and interferometry. MLI mosaics can be geocoded using the normal procedures used in the GAMMA Software. Typically, the S1 state vectors included with the data are of very accurate which results in geocoding accuracies better than a few meter, even without applying a refinement. Besides programs to extract SLC data of a single burst into an individual data file with a corresponding parameter file and programs to remove the azimuth spectrum variation related phase ramp from burst SLCs or SLCs of individual bursts are available.

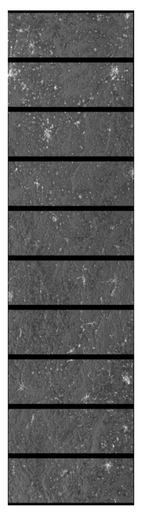

Figure 1 IW1 SLC bursts

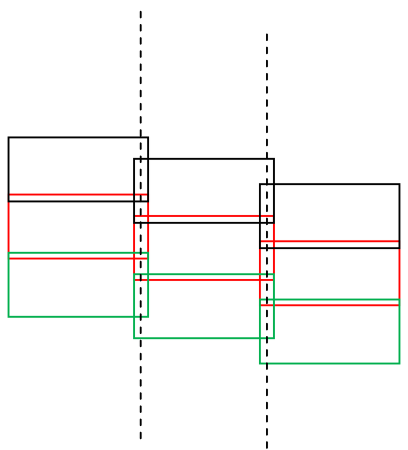

Figure 2 S1 burst structure with small overlaps between bursts and sub-swaths.

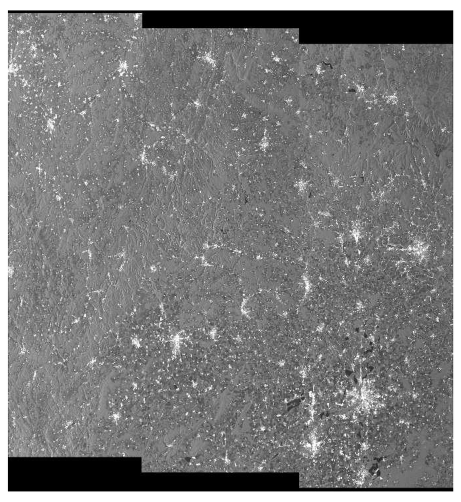

Figure 3 MLI mosaic for a "full S1 iWS" consisting of 3 sub-swaths with 10 bursts each.

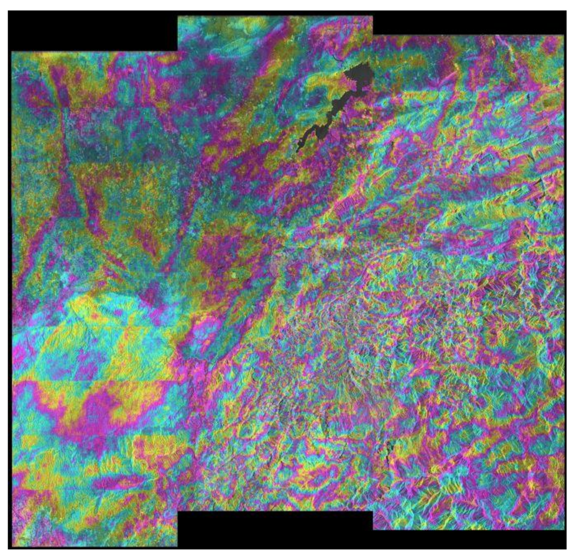

Figure 4 S1 TOPS differential interferogram as obtained using refined co-registration after the refinement using the matching procedure. One color cycle corresponds to one phase cycle. Phase jumps are clearly visible between some consecutive bursts.

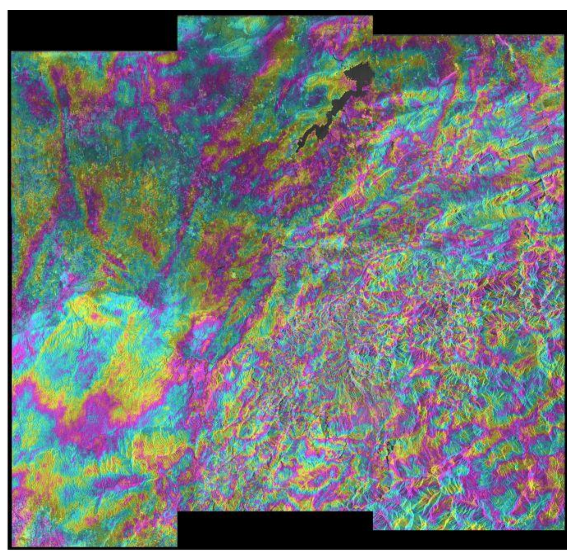

Figure 5 S1 TOPS differential interferogram as obtained after the spectral diversity co-registration refinement. One color cycle corresponds to one phase cycle. No more phase jumps are visible at the burst interfaces. The phase matches also well between adjacent sub-swaths.

S1 IWS Co-registration and Interferometry

For TOPS interferometry an extremely accurate co-registration in the azimuth direction is required [2] and therefore the refinement of the co-registration is done very carefully, using several methods and potentially iterating some of the steps to maximize the quality achieved. In the azimuth direction an accuracy of a few thousanths of a pixel is absolutely required, otherwise phase jumps between subsequent bursts are observed (Figure 4). To assure this very high co-registration accuracy we use a method that considers the effects of the scene topography. To determine the refinement of the transformation we typically use first a matching procedure and then a spectral diversity method [3] that considers the interferometric phase of the burst overlap regions. The refinement determined is only a constant offset in slant range and in azimuth (the same correction is applied for all bursts and sub-swaths).

A differential interferogram calculated after the refinement with the matching procedure (accuracy of the order of 1/100 azimuth pixel) is shown in Figure 4 and the final differential interferogram after refinement with the spectral diversity method is shown in Figure 5. Phase filtering, phase unwrapping (e.g. using a minimum cost-flow approach), phase to displacement conversion and coherence estimation are the same as for conventional stripmap interferometry.

Interferometric time series analysis

In the GAMMA IPTA Software a broad range of tools supporting different interferometric time series analysis approaches are supported, using either single or multi-looked interferometric phase and using either single reference or multi reference stacks to derive the deformation time series.

In the following the SBAS and PSI procedures used and the results achieved are discussed.

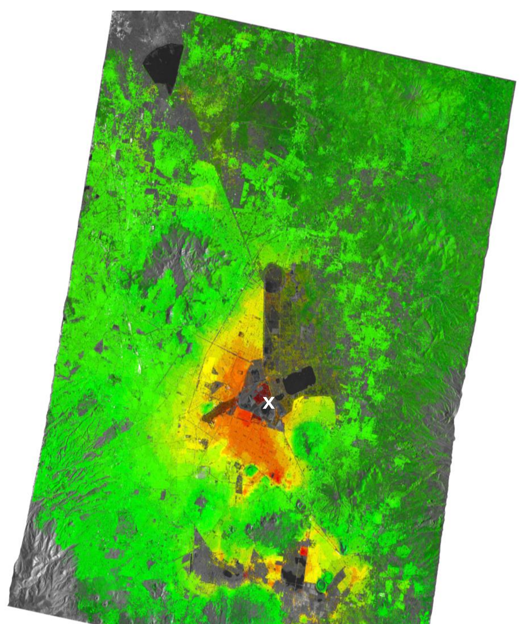

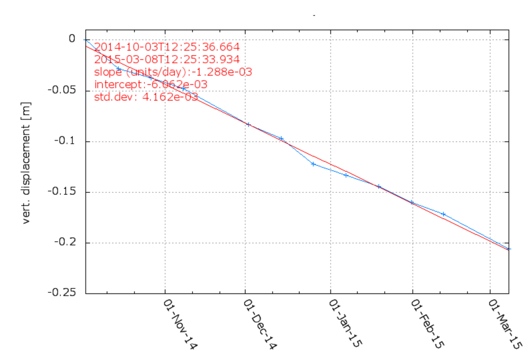

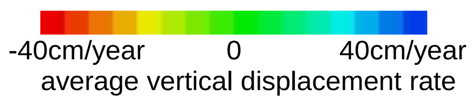

Figure 6 Average vertical displacement rate derived from 12 S1 IWS SLC over Mexico City using an **SBAS** procedure (color scale is indicated to the right)

Figure 7 Displacement history of an area near the international airport (see white **x** in Figure 6) derived using the described SBAS procedure.

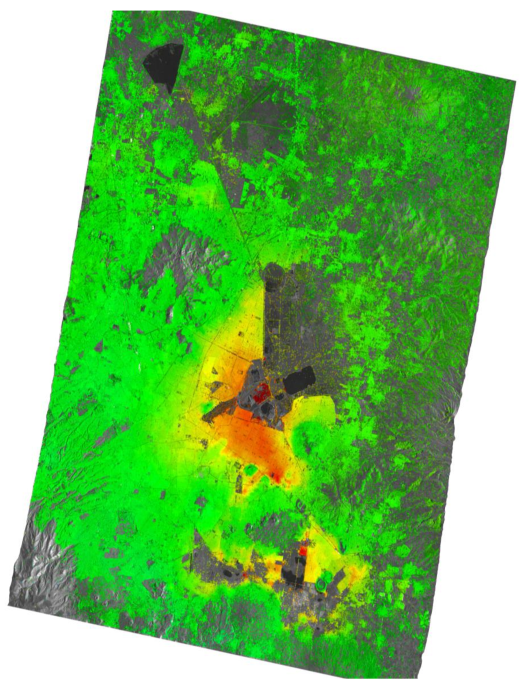

Figure 10 Average vertical displacement rate derived from a stack of 12 S1 IWS SLC over Mexico City using a **PSI** procedure (color scale is indicated above to the right).

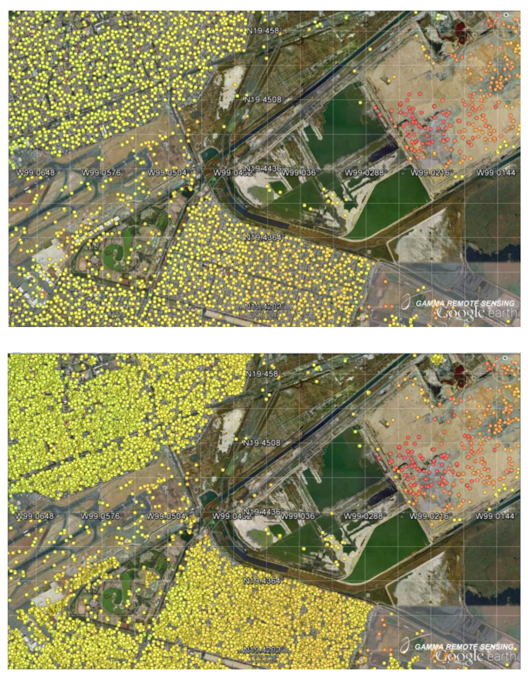

Figure 9 Local result of the S1v IWS PSI result over Mexico City (LOS displacement rates) in Google Earth with reduced (top) and full (bottom) point density.

S1 IWS offset tracking

To apply offset tracking for S1 TOPS mode SLC data the basic strategy is to first co-register the two burst SLC. In order to apply oversampling in the offset tracking procedures it is recommended to first deramp the SLC data for the azimuth phase ramp. Further processing (quality control, geocoding, conversion to displacements in meters, visualization) is then done as for normal stripmap mode data. An example of a glacier velocity map over a part of Greenland is shown in Figure 10.

For S1 TOPS mode GRD data offset tracking can be applied using the procedure as for strip-map mode data. The main interest in offset tracking is to map displacements. But azimuth offsets may also be of interest to identify ionospheric effects [6,7] or for radargrammetry.

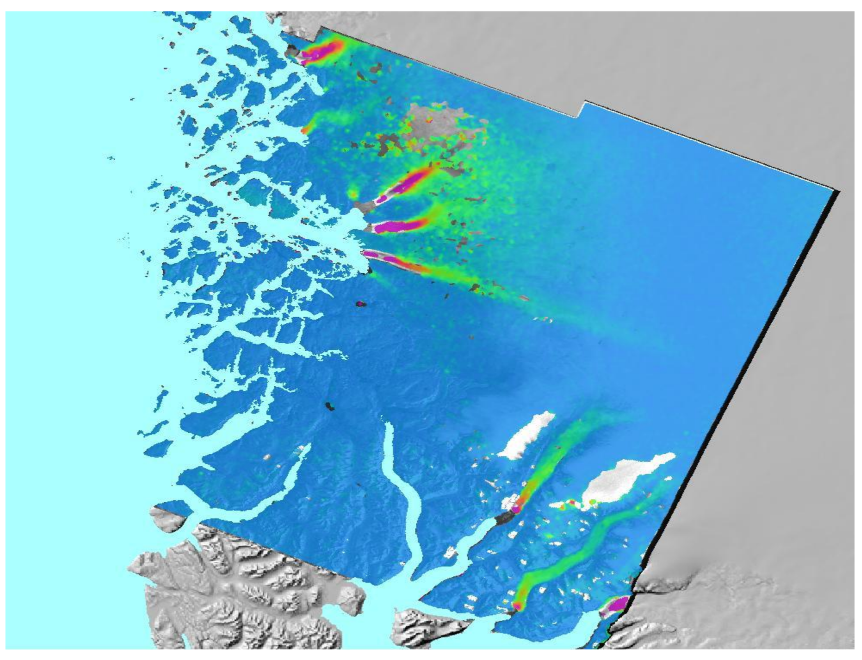

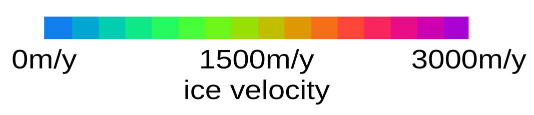

Figure 10 Velocity map of the Upernvaik area overlayed the shaded relief of the Greenland Mapping Project (GIMP) DEM [10]. Image width is about 250 km.

Conclusions

The procedures used in the GAMMA Software for interferometry, offset tracking and interferometric time series analysis (SBAS and PSI) using S1 IWS data were described. The main differences to "normal" strip map mode data are the organization of the IWS SLC data in 3 sub-swaths and by burst, the extremely accurate co-registration accuracy required for interferometry to avoid phase jumps between consecutive bursts (caused by the strong along-track Doppler Centroid variation). As a consequence much more care is taken with the co-registration procedure also including new elements as the use of a spectral diversity method applied to the burst overlap areas. The results achieved confirm that the S1 IWS data are well suited for interferometry, offset tracking and interferometric time series analysis.

S1 IWS Example over Mexico City

We used an S1 IWS SLC stack over Mexico City, consisting of 12 repeat observations. Because of the very significant ground motion in the Mexico City area we used multi-reference stacks for both the SBAS and PSI processing.

As input to the time series analysis we co-registered all the S1 IWS SLC to one selected reference scene (20151015). This was done using the procedure including the refinement with the spectral diversity method. The differential interferogram mosaics without visible phase jumps at burst interfaces and between sub-swaths and with generally very high coherence over urban areas confirm the high quality of the co-registration.. We deramped the co-registered SLC mosaics for the azimuth phase ramps and cut out a common 16000 x 5000 pixel section over Mexico city.

SBAS time series analysis with S1 IWS data

We followed an SBAS procedure similar to the one described in [8,9], considering multi-looked differential interferometric phases using 10 range and 2 azimuth looks. For the entire stack all the baselines were below 250m. To maximize the temporal coherence, to facilitate the phase unwrapping by minimizing the deformation phase, and including redundant observations we decided to include all pairs between scenes that are up to 3 positions away from each other in the time series (i.e. 1-2, 1-3, 1-4, 2-3, 2-4, 2-5, 3-4, …), which resulted in a total of 30 pairs. For each pair we calculated the differential interferogram using the SRTM height as topographic reference and unwrapped the phase. The unwrapped phases were then converted to a time-series using singular value decomposition (SVD, as supported in the program mb). Besides the phase time series quality information such as the phase standard deviation from the time series is determined. For areas where an unwrapping error occurred the phase standard deviation from the time series gets significantly higher and so the result in these areas could be excluded from the solution. The main results are the average deformation rate and the deformation time series (Figures 6,7). Converting the line-of-sight values to vertical displacement rates (assuming the movement is in the vertical direction) we observed maximum subsidence rates of up to more than 40cm/years. No anomalies were observed at the interfaces between subsequent bursts.

PSI time series analysis with S1 IWS data

The co-registered deramped SLC mosaic stack over Mexico City can be used as input to a PSI processing in the same way as used for conventional stripmap mode data. In the identification of persistent scatterer candidates, we applied a spectral diversity criteria as well as criteria on the backscatter variability and level [4]. Thanks to the good range resolution of the S1 IWS data a high number of suited persistent scatterers was identified. In urban areas the point density is typically larger than 1000 points/km^2. To make the PSI processing more efficient, we initially reduced the candidate list size using the methodology described in [5]. This is done adaptively, such that the point density is strongly reduced in areas with a very high point density while not reduced at all in areas with a low point density (Figure 9). The fact that only the vector data stacks are used in most IPTA programs means that the relevant parameter for the speed of a processing step is not the size of the area or of the full SLC but only the number of points in the point candidate list. This makes the IPTA approach very efficient for S1 IWS PSI. We used the same multi-reference stack as used in the SBAS processing. Using this multi-reference stack we estimated point height corrections, linear deformation rates and atmospheric phases. These initial linear deformation rate estimates are not of very high quality because they are based on the short interval pairs. The unwrapped phase components are then added to get the total point differential phases for the multi-reference stack. SVD is then used to convert the multi-reference stack phases to a single reference time series. Further processing may be done on this result considering the single reference stack. In this example this was not done because of the small stack size.

The average deformation rate derived in the PSI processing (Figure 8) corresponds closely to the result of the SBAS processing (Figure 6). Considering stable areas shows that mm/year precision is clearly not reached with this C-band stack of 12 scenes between October 2014 and March 2015. In these results (SBA and PSI) no anomalies were observed at the interface between subsequent bursts.

References

[1] De Zan F. and A. Guarnieri, Terrain Observation by Progressive Scans, IEEE Trans. Geosci. Remote Sensing, vol. 44, no. 9, pp. 2353-2360, 2006.
[2] Prats P., L. Marotti and R. Scheiber, Investigation on TOPS Interferometry with TerraSAR-X, Proc. of IGARSS 2010.
[3] Scheiber R. and A. Moreira, Coregistration of interferometric SAR images using spectral diversity, IEEE Trans. Geosci. Remote Sensing, vol. 38, no. 5, pp. 2179–2191, 2000.
[4] Werner C., U. Wegmüller, T. Strozzi, and A. Wiesmann, "Interferometric point target analysis for deformation mapping", Proc. IGARSS 2003, Toulouse, France, 21-25 July 2003.
[5] Wegmüller U., O. Frey, and C. Werner, "Point Density Reduction in Persistent Scatterer Interferometry", Procs. EUSAR 2012 Conf., 24-26. Apr. 2012.
[6] Wegmüller U., C. Werner, T. Strozzi, and A. Wiesmann, "Ionospheric electron concentration effects on SAR and INSAR", Proc. IGARSS 2006, Denver, Colorado, USA, 31- Jul. – 4. Aug. 2006.
[7] Wegmüller U., T. Strozzi, and C. Werner, Ionospheric path delay estimation using split-beam interferometry, Procs. IGARSS'2012, Munich, Germany, 22-27 July 2012.
[8] Berardino, P., Fornaro, G., Lanari, R., Member, S., & Sansosti, E., A New Algorithm for Surface Deformation Monitoring Based on Small Baseline Differential SAR Interferograms. IEEE TGRS, 40(11), 2375–2383, 2002.
[9] Lanari, R., Member, S., Mora, O., Manunta, M., Mallorquí, J. J., Berardino, P., & Sansosti, E., A Small-Baseline Approach for Investigating Deformations on Full-Resolution Differential SAR Interferograms. IEEE TGRS, 42(7), 1377–1386. 2004.
[10] Howat, I.M., A. Negrete, B.E. Smith, 2014, The Greenland Ice Mapping Project (GIMP) land classification and surface elevation datasets, *The Cryosphere*, 8, 1509-1518, doi:10.5194/tc-8-1509-2014.

This work was supported by the EC FP7 Projects CRYOLAND and SEN3APP.